High-Performance Video Condensation System

Jianqing Zhu, Shikun Feng, Dong Yi, Shengcai Liao, *Member, IEEE*,
Zhen Lei, *Member, IEEE*, and Stan Z. Li, *Fellow, IEEE*

***Abstract*— Video synopsis or condensation is a smart solution for fast video browsing and storage. However, most of the existing methods work offline, where two main phases are required. The first phase is to prepare tubes and background images. The second phase is to rearrange tubes and stitch them into backgrounds. However, with a long video sequence, the first phase is memory consuming for data storage, and the second phase is computationally expensive to rearrange all tubes simultaneously. To overcome these problems, we propose a high-performance video condensation system based on an online content-aware framework. The online framework transforms the optimization problem of tube rearrangement into a stepwise optimization problem. Therefore, it can condense video with much less memory and higher speed than the offline framework. With the aid of this transformation, the proposed system can process input videos and produce condensed videos simultaneously. Thus it is suitable for real-time endless surveillance videos. Meanwhile, the online mechanism allows users to directly visit the condensation video that has been generated. Moreover, the content-aware mechanism makes the proposed system able to automatically determine the duration of a condensed video. Finally, the proposed system uses Graphic Processing Unit (GPU) and multicore techniques to improve the speed. Extensive experiments that validate the high efficiency of the system are presented.**

***Index Terms*— GPU acceleration, moving object segmentation, online background generation, video condensation system, video storage, video surveillance.**

I. Introduction

IN THE past decade, there is an explosive growth of surveillance video data in the world. This situation brings about great demands for fast video browsing and storage technologies in public security field. However, how to fast browse and effectively extract useful information from the huge video data still remain challenging problems.

The easiest approaches about efficient browsing include fast forwarding [1] and video skimming [2]. In those methods, videos are fast browsed by skipping several frames between selected frames. However, skipped frames may cause important contents missing. The adaptive methods of skipping frames [3], [4] are thus proposed. Such methods skip frames in periods of low activity, while keeping frames in periods of high activity. A survey of fast video browsing is presented in [5]. Other approaches are video abstraction [6], [7], which use key frames as a synopsis to represent an original video. However, this key frame representation may lose the dynamic effect of a video sequence. A survey of video abstraction is given in [8]. Overall, the smallest processing unit of the above approaches is an entire frame, which means that they only condense original videos in time domain, but neglect redundances in spatial domain. Therefore, they cannot achieve high condensation ratio.

Alternatively, the space–time video montage [9] analyzes both the spatial and temporal information distribution of an original video. By taking the visually informative space–time portion as the smallest processing unit, it packs all these portions together to maximize the visual information of a condensed video. However, the video condensed by this method has obvious seams and information loss.

The ribbon carving-based method [10] considers a ribbon as the smallest processing unit. The so-called ribbon can be thought as a flexible frame without activity. This method repeatedly removes ribbons until there is no ribbon in an original video. However, its condensation ratio is low, and may fail when adjacent objects having different speeds and directions. Moreover, it always creates vertical or horizontal visible seams in condensed videos.

A significant progress in this field is video synopsis [11]–[13]. The goal of video synopsis is to produce a shortened video sequence by condensing an original video in temporal and spatial domains. As a tube (tube is a frame-sequence of an object)-based approach, video synopsis enables users to browse a day long video recording in just a few minutes by creating a summary of all activities. As shown in Fig. 1, the video synopsis framework includes the online phase and the response phase. The online phase is first performed to record background images and extract tubes from an original video using foreground segmentation and tracking algorithms. Therefore, this online phase is actually a preprocessing step used to collect tubes and backgrounds. In the response phase, an energy function is minimized to determine the play time of objects (tube rearrangement) in synopsis video and time-lapse background video is constructed, then the objects are stitched into the selected backgrounds to generate a synopsis video. Because the first phase is performed on the whole input video, therefore it is essentially an offline processing framework.

Manuscript received January 21, 2014; revised June 9, 2014 and August 13, 2014; accepted October 1, 2014. Date of publication October 17, 2014; date of current version June 30, 2015. This work was supported by the Chinese National Natural Science Foundation Projects #61203267, #61375037, #61473291, National Science and Technology Support Program Project #2013BAK02B01, Chinese Academy of Sciences Project No. KGZD-EW-102-2, and AuthenMetric R&D Funds. This paper was recommended by Associate Editor A. Signoroni. *(Corresponding author: Stan Z. Li.)*

J. Zhu is with the National Laboratory of Pattern Recognition, Center for Biometrics and Security Research, Institute of Automation, Chinese Academy of Sciences, Beijing 100190, China, and also with the Faculty of Software, Fujian Normal University, Fuzhou, 350108, China (e-mail: jqzhu@cbsr.ia.ac.cn).

S. Feng, D. Yi, S. Liao, Z. Lei, and S. Z. Li are with the National Laboratory of Pattern Recognition, Center for Biometrics and Security Research, Institute of Automation, Chinese Academy of Sciences, Beijing 100190, China (e-mail: szli@cbsr.ia.ac.cn).

Color versions of one or more of the figures in this paper are available online at http://ieeexplore.ieee.org.

Digital Object Identifier 10.1109/TCSVT.2014.2363738

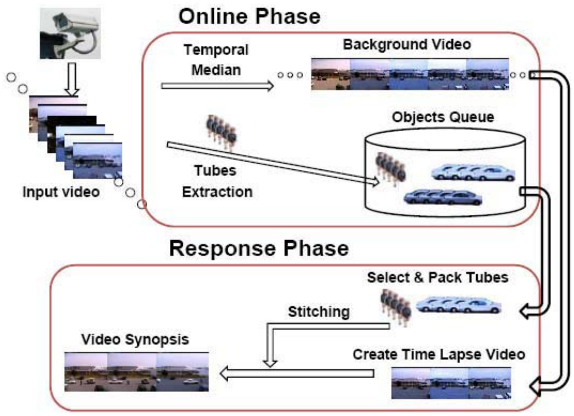

Fig. 1. Framework of video synopsis [11]. The image is derived from [11]. It is essentially an offline framework because it relies on a preprocessing step performed in the first phase.

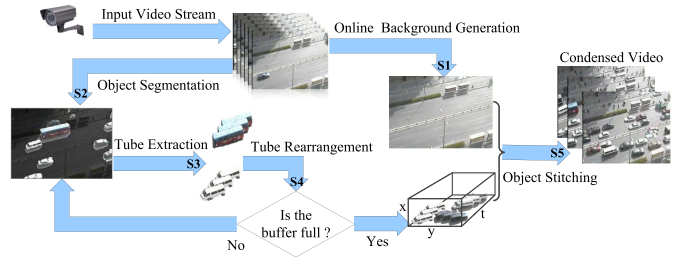

Fig. 2. Online content-aware video condensation framework. This framework does not need any preprocessing step. Based on a memory buffer, it can parallelly perform S4 and S5, thus can process an input video and generate the condensed video simultaneously.

Following the video synopsis framework, several improved methods are proposed in [14]–[16]. These methods have achieved some improvements with respect to speed or tube rearrangement effect. However, this two-phase offline framework still has some drawbacks when it handles a very long video sequence.

1) It needs huge memory to store all tubes and backgrounds first or have to delete some objects.
2) Its processing speed is low, because it deals with all data in one time.
3) Its query efficiency is low, because it must perform tube rearrangement and object stitching algorithms to generate the corresponding synopsis video for each query.
4) The duration of a synopsis video is determined manually rather than by the content of an input video, which is impractical because users may not know the activity density of an input video beforehand.

To overcome the drawbacks of huge memory cost and slow speed when the offline framework deals with long videos, the most direct way is to manually divide a long input video into several short sequences, and then use the offline framework to process each short sequence. However, in practice, this method may face two problems: 1) an object's trajectory may be divided into different sequences, which will degrade user experience, and 2) different sequences usually have a different activity density, which makes it difficult for users to determine an adequate length for each synopsis video.

In this paper, a high-performance video condensation system is proposed to overcome the mentioned drawbacks. This paper is built upon our preliminary work: online content-aware video condensation framework reported in [17]. The online content-aware video condensation framework transforms the optimization problem of tube rearrangement in traditional video synopsis approaches into a stepwise optimization problem. The main novelty of this framework is the online processing manner, which is able to keep processing a long input video while at the same time incrementally produces condensed video. As shown in Fig. 2, our online framework only includes one phase, which does not need a preprocessing step used to prepare tubes and background images.

To construct a more practical video condensation system, a number of techniques are introduced in this paper to enhance the system on speed and memory consumption, including:

1) *An Online Background Generation Method*: This method generates a time-lapse background image by averaging frames in a time interval and updates it over time. The memory cost of this method is low and the produced background can reflect the background changes over time.
2) *A Faster Moving Object Segmentation Method*: The scale invariant local ternary pattern (SILTP) feature-based background subtraction algorithm [18] is applied to achieve effective moving object segmentation.
3) *A Multithread Implementation Framework*: The online content-aware video condensation framework is divided into tube generation, tube rearrangement, and object stitching modules, which are parallelly implemented.
4) *An Effective Memory Buffer Design*: The memory buffer is based on the producer–consumer model used to control the memory balance between different multithread modules of the system.
5) *GPU and Multicore Acceleration Strategies*: The GPU and multicore techniques are used to accelerate the processing speeds of SILTP-based moving object segmentation and object stitching, respectively.

The advantages of the high-performance video condensation system will be validated by experiments, which are summarized as follows.

1) *Fast Speed:* On an eight cores 2.66-GHz computer with a GPU (Nvidia GeForce GTX 285), the system processing speed achieves 530–660 frames/s for videos with 320×240 resolution, and even for high resolution (704×576) videos, it achieves 100 frames/s.
2) *Low Memory Cost:* The system can online processing videos, which does not require huge memory to preserve all tubes and backgrounds.
3) *High Condensation Ratio:* The system can achieve a higher condensation ratio than the ribbon carving-based method [10].
4) *High Query Efficiency:* In each query, the system allows users to directly obtain the condensed videos that have been generated rather than executing tube rearrangement and object stitching each time.
5) *Ability to Process Endless Video:* The system can process input videos and produce condensed videos

simultaneously, thus it is able to deal with real-time endless surveillance video.

6) *Adaptivity:* The system can produce a condensed video with adaptive condensation ratio. This is more reasonable than setting by manual as in [11].
7) *Compatibility:* The system is able to condense videos in offline or online modes.

The rest of this paper is organized as follows. Section II describes the details of the online content-aware video condensation framework, including online background generation, moving object segmentation, sticky tracking, tube rearrangement, and object stitching, respectively. Section III introduces the high-performance system, including software design and acceleration strategies. Section IV presents experimental results to show the superiority of the proposed system. Section V concludes this paper.

II. Online Content-Aware Video Condensation Framework

A. From Offline to Online

The smallest processing unit of video synopsis is tube. A tube is defined as the frame sequence of the same object in a video. The main idea of video synopsis is to remove activity-less frames, and rearrange tubes in video frames to make objects that appear sequently in an original video can appear simultaneously in the shortened video. As shown in Fig. 1, the video synopsis framework includes two phases. The online phase is first performed in real time during video capturing and recording. The response phase is performed following a user query to generate synopsis videos. The online phase can be seen as a preprocessing step for an original video to prepare tubes and backgrounds, which must be performed first, and then a synopsis video is produced in the respond phase, which needs a user query. Consequently, it is essentially an offline framework because a synopsis video is produced until a preprocessing step was performed in the first phase.

Let us focus on the response phase where tubes are rearranged in temporal domain. Assuming that tubes and backgrounds have been prepared, then the problem of tube rearrangement can be viewed as a constrained optimization problem. Tube rearrangement is to reassign the start-time label of each tube so that multiple tubes originally appearing in different times can be displayed simultaneously under some constraints. The constraints proposed in [11] include keeping maximum activity, consistency with background, keeping chronological order, and avoiding collisions (occlusions) between tubes. The optimization problem can be formulated as minimizing the following energy function:

$$E(\ell) = \sum_{i \in \boldsymbol{Q}} E_u(\ell_i) + \alpha \sum_{i,j \in \boldsymbol{Q}} E_p(\ell_i, \ell_j) \tag{1}$$

where $\boldsymbol{Q}$ denotes the whole tube set and ℓ_i denotes the start-time label of tube i, which takes a value from the time label set

$$\mathcal{L}_{\text{Offline}} = \{1, \ldots, M\} \tag{2}$$

where M denotes the number of frames in a condensed video and is actually set by users. E_u and E_p denote the unary and pairwise energy functions, respectively. α is used to control the weight of the pairwise energy function E_p. Specific formulations of E_u and E_p will be discussed later. We can find that, the optimization of (1) involves all tubes in one time. Minimizing such problem is very time-consuming when $|\boldsymbol{Q}|$ or M is huge. Besides that, it requires much room to prepare all tubes and backgrounds. For example, the memory cost of a video sequence with 10 h duration (30 frames/s $\times$ 3600 s $\times$ 10 $=$ 1 080 000 frames, 320 $\times$ 240 pixel resolution, and three channels) is 1 080 000 $\times$ 320 $\times$ 240 $\times$ 3 $\times$ 8bit $\approx$ 232 GB. Assuming that the foreground pixel ratio is 1% and backgrounds are recorded with a 10-frame interval, therefore, the offline framework must cost 232 $\times$ 1% $=$ 2.32 GB to save tubes and 232 $\times$ 0.1 $=$ 23.2 GB to save backgrounds, respectively. In other words, the offline framework has the drawbacks of slow speed and huge memory cost when it deals with long videos.

The online content-aware video condensation framework is used to overcome the drawbacks in the offline framework. As shown in Fig. 2, the online framework only includes one phase, rather than two phases. It consists of five main steps:

1) *S1 (Background Image Generation):* Generate a background image using the online background generation method.
2) *S2 (Moving Object Segmentation):* Segment moving objects using the SILTP feature-based background subtraction algorithm [18].
3) *S3 (Tube Extraction):* Extract tubes using the sticky tracking algorithm.
4) *S4 (Tube Rearrangement):* Decide optimal start-time labels of tubes using the online tube filling algorithm and push the rearranged tubes into a memory buffer.
5) *S5 (Object Stitching):* If the buffer is full, stitch tubes in this buffer into the background image (S1) using the modified Poisson image editing method [11].

Note that, based on a memory buffer, the online framework is able to parallelly perform S4 and S5, which can process an input video and generate the condensed video simultaneously. Therefore, it is a real online video condensation framework.

The online property of the online content-aware framework is first discussed, and the content-aware property will be discussed later. The basic idea of the online framework is to transform the optimization problem of (1) into a stepwise optimization problem of (3), which only involves a subset of the whole tube set; that is, it determines the start-time label of each tube in the subset one-by-one. For the current tube i, its start-time label ℓ_i is calculated by minimizing energy function

$$E(\ell_i) = E_u(\ell_i) + \alpha \sum_{j \in \boldsymbol{Q}'} E_p(\ell_i \mid \ell_j) \tag{3}$$

where $\boldsymbol{Q}' \subset \boldsymbol{Q}$ denotes the subset of processed tubes; $\ell_{(\cdot)}$ takes a value from a much smaller label set

$$\mathcal{L}_{\text{Online}} = \{1, \ldots, n\} \tag{4}$$

where n denotes the number of frames in a temporary condensation space, with $n \ll M$. ℓ_j is the known start-time label of the processed tube j. The optimization of (3) deals with a tube subset at each step, which is a good approximation to the optimal solution of (1). However, compared with (1), the label set of (3) is much smaller ($n \ll M$) and the number of involved tubes is fewer ($|Q'| < |Q|$), which significantly reduces the time cost of tube rearrangement. Moreover, there is no need to store all tubes $\boldsymbol{Q}$ in memory but just a subset $\boldsymbol{Q'}$. Therefore, the optimization of (3) can achieve high speed with low memory cost.

B. Online Background Generation

A condensed video sequence consists of tubes and backgrounds; that is, each frame in a condensed video sequence is generated by stitching moving objects into a background image. In practice, the number of frames in a condensed video M is much smaller than the number of frames in the corresponding original video N ($M \ll N$). Therefore, a background selection mechanism is needed in video condensation application.

The selected background images should meet two properties [12]: 1) Property-I, it should reflect background changes over time, such as the alternation of day and night and 2) Property-II, it should be related with video activities; that is, backgrounds containing more moving objects are preferred. The two properties are conflicting. To address this tradeoff, [12] combines two temporal histograms with a weight to meet the two properties. However, this method is an offline approach, which needs to store all N backgrounds first, requiring huge storage space. To reduce storage cost, the online principal background selection (OPBS) method is proposed in [19]. As an online version of background selection method, the OPBS method needs to store n backgrounds ($n < M \ll N$, a typical value is $n = 500$).

In this paper, an online background generation method is proposed to coordinate with the online framework. It generates a background image by averaging frames in a time interval (in our experiments, set this time interval to be 3000 frames) and updates it over time. The advantage of this method is that it only needs to store one background image.

The background image generated by this simple method still meets the two properties under the online content-aware video condensation framework. Because it is updated over time, therefore, it naturally meet Property-I. As discussed above, the tube rearrangement is realized in a stepwise way, thus the corresponding condensed video is produced in a stepwise way too. In each step, a set of tubes are stitched into a generated background image. In the period that contains more activities the online content-aware framework is more likely to trigger stitching operation (this is called content-aware ability of the online framework, which will be discussed later) to produce stitched frames that in a condensed video, thus background images that appear in the period with more activities are more often to be used in the condensed video. Therefore, it also meets Property-II.

C. Moving Object Segmentation

Because the smallest processing unit of video condensation is tube, the moving object segmentation must be performed before tube extraction. In [11] and [17], a graph cut (GC)-based object segmentation method is used to obtain a smooth segmentation of moving objects. The GC-based object segmentation method used in [11] and [17] is a simplification of background cut [20]. In [17], the color-based unary term is the color difference between the current image and the estimated background image and the background image is produced using the mixture of Gaussian (MoG) [21] method. Since the GC-based object segmentation method is computationally expensive, the multithread GC method is proposed in [17] to accelerate the processing speed.

TABLE I

ACCURACY COMPARISON BETWEEN THE SILTP [18] AND GC-BASED [17] OBJECT SEGMENTATION METHODS. THE TEST VIDEO SEQUENCES COME FROM CHANGE DETECTION 2014 [22]

Sequence	Recall(%)		Precision(%)		F-score(%)	
	SILTP	GC	SILTP	GC	SILTP	GC
highway	**95.87**	95.65	**59.03**	56.81	**73.07**	71.28
PETS2006	**97.08**	91.59	**54.19**	35.18	**69.56**	50.83
pedestrians	**95.22**	86.67	37.72	**46.68**	54.04	**60.68**
peopleInShade	**98.96**	97.64	**55.68**	46.90	**71.26**	63.37
Average	**96.78**	92.89	**51.66**	46.39	**66.98**	61.54

In this paper, the SILTP feature-based background subtraction algorithm [18] is applied to achieve effective moving object segmentation. As reported in [18], the SILTP feature-based background subtraction method can achieve better segmentation results than the MoG approach [21], whereas the processing speed of SILTP is comparable with that of MoG.

Here, we also report a comparison of the SILTP [18] and the GC-based [17] object segmentation methods. The accuracy comparisons are shown in Table I, where $\text{Recall} = \text{TP}/(\text{TP} + \text{FN})$, $\text{Precision} = \text{TP}/(\text{TP} + \text{FP})$, and $\text{F}-\text{score} = 2 \cdot \text{Recall} \cdot \text{Precision}/(\text{Recall} + \text{Precision})$. TP, FP, and FN are true positives (true foreground pixels), false positives, and false negatives (false background pixels), respectively.

From Table I, we can find that both SILTP and GC-based object segmentation methods achieve high recall rates. This shows they can completely segment moving objects. Moreover, the precisions of SILTP-based method are higher than that of the GC-based method in most cases; therefore, the SILTP-based method has better F-score performance. However, the precision rates of the two methods are relatively low. This is resulted from a conservative background decision threshold setting, which favors more foreground pixels so that the extracted objects will be complete for video condensation. The segmentation results of SILTP and GC-based methods are shown in Fig. 3, where we can see that both of the two methods can completely segment moving objects. However, the GC-based algorithm used in [17] sometimes causes obvious under-segmentation because the color difference-based unary term is sensitive to illumination variations, whereas the SILTP-based method has a better segmentation due to its illumination invariant nature in design. Furthermore, we propose a GPU accelerated SILTP-based moving object segmentation method, which will be described in Section III-C1, with a processing speed comparison with [17].

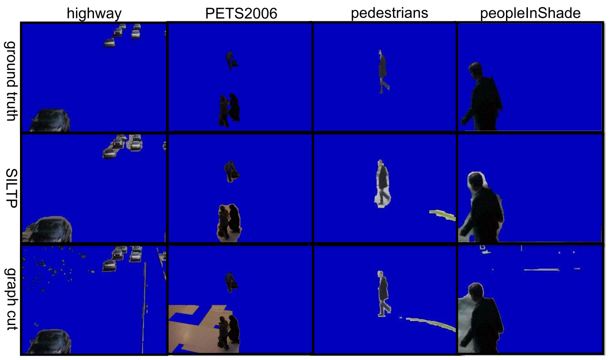

Fig. 3. Segmentation results of SILTP and GC-based methods.

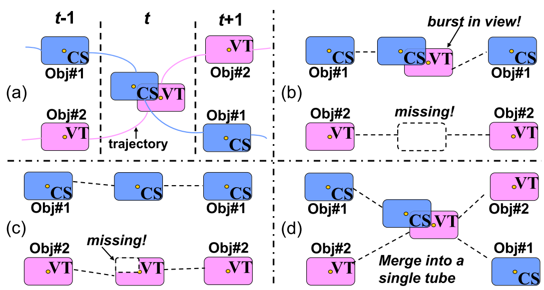

Fig. 4. Occlusion between two objects. See Section II-D for details.

D. Sticky Tracking

If moving objects have been segmented, a tracking algorithm is applied to connect the same object appearing in different frames for tube extraction. Many tracking methods [23], [24] have been proposed, however, those methods may not be entirely suitable for video condensation. The following example shows the problems. As shown in Fig. 4(a) with two objects, where Obj#2 is occluded by Obj#1 at frame t. Fig. 4(b) shows the result of a common blob tracking method [24]: two tubes are generated, but both are not good enough. Because the merged blob is matched to Obj#1 at frame t, something not belonging to Obj#1 will burst into view in a condensed video. Meanwhile, no blob is matched to Obj#2. Obj#2 will disappear abruptly and then appear again in the view. As a result, both tubes will cause a blinking effect, thus deteriorating user experience. Fig. 4(c) is the result of an ideal tracking method that produces the most accurate result. However, such an optimal tracker is not completely suitable for video condensation application: part of Obj#2 is lost due to the occlusion at frame t, which also causes blinking.

The sticky tracking strategy is used to reduce blinking effect in a condensed video for better visual effects. It is based on the following idea: if occlusions happen to two or more tubes, they will be merged into a single tube, as if they are sticking together in Fig. 4(d). Note that the goal of sticky tracking is very different with that of traditional tracking methods. The key point is to launch merging before matching. That is, if two or more tubes in the object list are matched to the same blob by the nearest object center distance at frame t, the two tubes will be merged and treated as one tube from frame t on.

In addition to reducing the blinking effect caused by occlusions between objects, sticky tracking presents another advantage, being able to amend poor object segmentation (under-segmentation and over-segmentation). The case of under-segmentation can be treated as object occlusion, which can be solved by sticky tracking. Fig. 5 shows some sticky tracking results for the other case of over-segmentation.

Fig. 5. Some sticky tracking results. (a) The head and the body of the same person were considered as two objects due to the over-segmentation at frame 732. When the segmentation becomes correct at frame 733, the head and body are merged into a single tube using sticky tracking. (b) One person with a suitcase splits into two objects at frame 4548 due to occlusions by the fence, and sticky tracking still successfully considers them as the same object. If two or more parts have the same color, they are considered as a single tube.

Moreover, sticky tracking has an ability to keep the chronological order of objects when they are close to each other (e.g., taking a conversation): if the distance between objects is less than a threshold (10 pixels in our experiments), they will be merged into one tube by sticky tracking, therefore, their chronological order will be naturally preserved.

E. Tube Rearrangement

The role of tube rearrangement is to decide each tube's start-time label. The online content-aware tube filling algorithm is the core of tube rearrangement. The main idea of online tube filling comes from the Tetris game, suggesting to deal with tubes one-by-one, rather than all in one time as in [11]. In Tetris, a player is encouraged to manipulate the Tetris to create a horizontal line without gaps, and then such line can be cleared. If the player is smart enough, the game can go on forever. Similarly, the online tube filling algorithm treats tubes as Tetris, and regards a 3-D condensation space as the playing field of video condensation. If the playing field is saturated, the rearranged tubes are pushed into the object stitching stage and so the current playing field is cleared. In the following, our job is to design a smart player for the tube filling game.

1) Objective Function Construction: In (1) and (3), the objective functions consist of unary and pairwise energy functions. In [11], the unary energy function includes activity cost (the penalty of losing tubes in a condensed video) and background inconsistency cost (the penalty of the inconsistency among tubes and background images), whereas the pairwise energy function includes collision cost (the penalty of occlusion between tubes) and temporal consistency cost (the penalty of the temporal inconsistency between tubes). Based on these four cost terms, it is time consuming to find an optimal solution for (3); therefore, according to the characteristics of the online content-aware framework, we define a simplified objective function

$$E(\ell_i) = \sum_{j \in \boldsymbol{Q}'} E_c(\ell_i \mid \ell_j) \tag{5}$$

where $E_c(\cdot|\cdot)$ represents the collision cost between two tubes, and its definition will be discussed later.

First, we can find that (5) does not include the unary energy function $E_u(\cdot)$, where it is set as $E_u(\cdot) \equiv 0$. The motivations are follows: 1) considering the activity cost is to punish the case that some tubes disappear in a condensed video, therefore, if all tubes are forcibly stitched into the condensed video, there is no need to consider the activity cost and 2) the background inconsistency among tubes and background images is not significant in the online framework. Because the background image generation and tube rearrangement both are performed in online way that the time difference between rearranged tubes and background image is not too large, therefore, there is no need to consider the background inconsistency cost.

Second, we can find that only the collision cost is considered in (5). The motivation is that the temporal inconsistency between tubes is not remarkable in the online framework where the tube rearrangement is performed in a stepwise way; that is, rearranged tubes are extracted from a short interval at each step. Besides that, the start-time label set $\mathcal{L}_{\text{Online}}$ is small so that it can not produce serious temporal inconsistency between two tubes.

In [11], the collision cost is defined as the volume of two tubes' space–time overlap weighted by their activity measures. However, this cost function is insufficient because it is prone to ignore small tubes. Since a small tube contributes a tiny penalty in the overall energy function, it may be completely occluded by other tubes. To overcome this drawback, a new collision cost will be necessary to give a high penalty for this case.

Assuming a current tube i and a rearranged tube $j \in \boldsymbol{Q'}$ are placed at the location ℓ_i and ℓ_j, respectively. Then, the collision cost function $E_c(\ell_i \mid \ell_j)$ is defined as

$$E_c(\ell_i|\ell_j) = \sum_{t \in t_i \cap t_j} e^t(i, j) \tag{6}$$

$$e^t(i, j) = \begin{cases} s^t_{i,j}, & \dfrac{s^t_{i,j}}{I^t(i, j) \cdot a^t_j + (1 - I^t(i, j)) \cdot a^t_i} < \beta \\ \kappa \cdot a^t_i, & \text{otherwise} \end{cases} \tag{7}$$

where $t_i \cap t_j$ is the temporal intersection of tube i and j in the condensation space, $e^t(i, j)$ denotes the collision cost between tube i and a rearranged tube j at frame t, a^t_i and a^t_j denote the area of tube i and j at frame t, respectively, $s^t_{i,j} \in [0, \min(a^t_i, a^t_j)]$ denotes the area intersection between tube i and j at frame t, $\beta \in [0, 1]$ denotes the maximal tolerable occlusion ratio, and $I^t(i, j)$ is an indicator used to designate the depth ordering of tube i and j at frame t: if tube i is closer to the camera than tube j, which means tube i may occlude tube j, then $I^t(i, j) = 1$; otherwise, $I^t(i, j) = 0$. As shown in Fig. 6, tube i occludes tube j, while it is occluded by tube k at frame t. In this case, $I^t(i, j) = 1$ and $I^t(i, k) = 0$. Such depth ordering of tubes, which determines the relationship of occlusion, can be obtained by a simple ground plane heuristic [12]. See [25] for more about depth ordering.

With (7), no matter the size of tube i, once the occlusion ratio of the corresponding slice t of tube i is higher than β which indicates the rearrangement of tube i will cause serious occlusion, then it should be heavily penalized, and the strength of penalty depends on the coefficient κ.

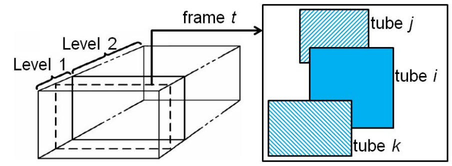

Fig. 6. Collision situations of tube i, j, and k at frame t.

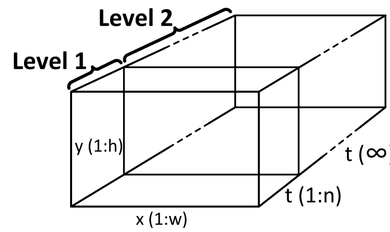

Fig. 7. Two-level condensation space.

2) Two-Level Condensation Space: The two-level condensation space is used as the playing field of the tube filling game. As show in Fig. 7, it includes two level with different size: the size of the first-level condensation space $L1$ is $w \times h \times n$, whereas the size of the second-level condensation space $L2$ is $w \times h \times \infty$, where w and h denote the width and height of the input video frames, and n [same as in (4)] denotes the number of frames in the $L1$ condensation space. The tube set $\boldsymbol{Q'}$ in (3) is made of tubes in the $L1$ condensation space.

The $L1$ condensation space is the real playing field of the tube filling game. That is to say, the start-time label of an incoming tube should be confined in the $L1$ condensation space. Besides, the function of the $L2$ condensation space is to receive the tail of the incoming tube if $L1$ condensation space can-not hold the whole tube.

As the $L1$ condensation space receives more-and-more tubes, it will be full at some point, just like creating a horizontal line of blocks without gaps in the Tetris game. At this time, the content of the $L1$ condensation space is stitched to a background image for producing condensed video, then the $L1$ condensation space will be cleared and the first n frames of $L2$ condensation space will be pushed into the $L1$ condensation space. That is to say, the tube set $\boldsymbol{Q'}$ is set to $\boldsymbol{Q''}$ at this time, where $\boldsymbol{Q''}$ is the tube tails whose start-time labels have been set as 1. This mechanism is able to keep the chronological order of tubes even they may not be filled into the same $L1$ condensation space in one time.

Note that, both $L1$ and $L2$ condensation spaces are logical spaces rather than real physical memory spaces; that is, rearranged tubes are stored in the rearranged tube buffer, which will be introduced in Section III-B.

3) Online Content-Aware Tube Filling: There are two main tasks for the online content-aware tube filling algorithm: 1) deciding each tube's optimal location in the $L1$ condensation space and 2) deciding whether the $L1$ condensation space is saturated. For the first, a greedy optimization method is used to decide each tube's optimal location. For the second, tubes with high collision ratio are saved in a temporary list,

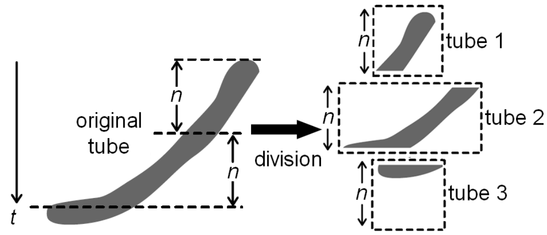

Fig. 8. Tube division.

once the length of the temporary list surpasses a threshold, the $L1$ condensation space is considered as saturated.

Based on (5)-(7), the optimal location $\mathscr{L}(i)$ of tube i is found by greedy search, as

$$\mathscr{L}(i) = \arg\min_{\ell_i} \sum_{j \in \boldsymbol{Q}'} E_c(\ell_i \mid \ell_j) \tag{8}$$

where $\ell_{(\cdot)} \in \{1, 2, \ldots, n\}$. The optimal location is found according to the locally optimal choice at each greedy search step with the hope of making the $L1$ condensation space full with least collision at last.

A content-aware mechanism is further designed to accomplish the second task. The following criterion is used to decide if tube i can be filled into the $L1$ condensation space:

$$\mathcal{CR}_i(\mathscr{L}(i)) > \tau \tag{9}$$

where τ is the maximum tolerable threshold and the collision ratio $\mathcal{CR}_i(\mathscr{L}(i))$ of tube i is defined as

$$\mathcal{CR}_i(\mathscr{L}(i)) = \sum_{j \in \boldsymbol{Q}'} E_c(\mathscr{L}(i) \mid \ell_j) \Big/ \sum_{t \in t_i} a_i^t \tag{10}$$

where a_i^t denotes the area of tube i at frame t and t_i denotes the frame length of tube i. The tube i can not be filled into the $L1$ condensation space if its collision ratio $\mathcal{CR}_i(\mathscr{L}(i))$ larger than the maximum tolerable threshold τ, then such tube will be added to a temporary list $\boldsymbol{D}$, and the $L1$ condensation space is assumed to be saturated once the length of this temporary list reaches to the maximum temporary list size m. The benefit of this content-aware mechanism is that the duration of a condensed video is determined by the content of the input video, rather than by users as in [11].

4) Tube Division: Tube division is used to produce the dynamic stroboscopic effect [11]: the same object from different frames in an original video may be displayed at the same frame in the corresponding condensed video. It is simply achieved by dividing a tube into several smaller tubes, and the size of each one after division is guaranteed to be smaller or equal to the number of frames n in the $L1$ condensation space. See Fig. 8 for an example.

Tube division may cause the blinking effect and is not favorable in the online video condensation algorithm. However, with it the online video condensation algorithm can achieve higher condensation ratio.

5) Computational Cost Analysis: Assume that the computational cost of (6) is c; the start-time label set of online and offline tube filling are $\{1, 2, \ldots, n\}$ and $\{1, 2, \ldots, M\}$, respectively; the $L1$ condensation space saturated count is k, then we have $M = kn$; there are P tubes to be rearranged. Furthermore, we assume the $L1$ condensation space includes p tubes at each saturated moment, thus we have $P = kp$. With greedy search (8), the computational cost of online and offline tube filling is $k \cdot n(p-1)p/2c$ and $M(P-1)P/2c$, respectively. Therefore, their ratio is

$$\frac{k \cdot n \dfrac{(p-1)p}{2} c}{M \dfrac{(P-1)P}{2} c} = \frac{k \cdot n \dfrac{(p-1)p}{2} c}{kn \dfrac{(kp-1)kp}{2} c} \approx \frac{1}{k^2}. \tag{11}$$

F. Object Stitching

The rearranged tubes are stitched into backgrounds using the modified Poisson image editing [11] according to the corresponding start-time labels. See [11] for more details about the modified Poisson image editing.

III. High-Performance Video Condensation System

A. Multithread-Based System

The online content-aware video condensation framework includes three primary modules: 1) tube generation module, including online background generation, moving object segmentation, and sticky tracking and 2) tube rearrangement module and 3) object stitching module. As shown in Fig. 9, these modules are paralleled performed by the tube generation thread, the tube rearrangement thread, and the object stitching thread, respectively. The relationship between the tube generation thread and the tube rearrangement thread can be seen as the relationship between producer and consumer. The tube generation thread just like a tube producer that pushes tubes into a tube buffer, whereas the tube rearrangement thread like a consumer that gets out tubes from the tube buffer for online tube filling. The detail of this producer–consumer parallel model is introduced in [26]. Similarly, there is also a producer–consumer relationship between the tube rearrangement thread and the object stitching thread. However, in this case, the tube rearrangement thread is a producer and the object stitching thread is a consumer.

Note that, the system is compatible with offline video synopsis [11]–[13] by a slight adjustment. Specially, one can trigger the tube generation thread first to extract all tubes and backgrounds from an input video sequence, and then trigger the tube rearrangement thread to rearrange all tubes, at last trigger the object stitching thread to generate a condensed video. Note that, tubes are still rearranged using (8), however, the system must prepare all tubes and backgrounds existing in the input video sequence in this case.

B. Buffer Design

As shown in Fig. 9, there are two memory buffers in the proposed system. The tube buffer used between the tube generation thread and the tube rearrangement thread is an first in first out (FIFO) list. The element of this FIFO buffer is a tube that waiting to be rearranged. The rearranged tube buffer used between the tube rearrangement thread and the object stitching thread is also a FIFO list. To avoid the efficiency

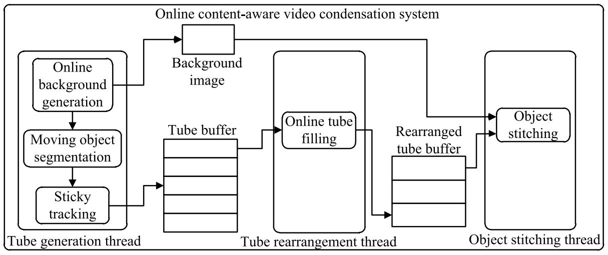

Fig. 9. Structure of the online content-aware video condensation system.

deterioration caused by the frequent data interaction between the tube rearrangement thread and the object stitching thread, the element of the rearranged tube buffer is designed to store multiple rearranged tubes. Adjusting the length of the two buffers can balance the speed and memory usage of the proposed system.

C. Acceleration Strategies

In Fig. 9, moving object segmentation and object stitching are the most time-consuming steps. To achieve faster processing speed, the GPU-based moving object segmentation and the multicore-based object stitching are proposed.

1) GPU-Based Moving Object Segmentation: Traditional background subtraction methods, such as the MoG approach [21], are usually based on the color of pixels, and each pixel is processed independently. This makes the mixture of Gaussian approach a highly parallelable algorithm, which can be easily accelerated by GPU. However, the SILTP [18] pattern of each pixel is related to its four neighborhood; therefore, SILTP is harder to be parallelized on GPU. However, there are many tricks introduced in [27] can be used to parallelize the SILTP method. The SILTP is optimized in three aspects: 1) pinned memory; 2) memory coalescing; and 3) asynchronous execution.

The bandwidth between host memory and device memory is usually a bottleneck in GPU computation. As suggested in [27], pinned memory can help to improve the speed of data transfer between host memory and device memory, hence, the pinned memory is used. Furthermore, using pinned memory allow us to launch the SILTP algorithm asynchronously. In Compute Unified Device Architecture (CUDA), when 16 continuous threads in the same block access continuous global memory, all individual transfers will be combined into a single transfer automatically, which is called memory coalescing [27]. To take this advantage, the distribution of the neighborhood pixels to the threads is designed from a same block as possible. In the calculation of SILTP pattern for each pixel, it always access the four neighborhood in a block. However, the four pixels are not continuous in global memory. Therefore, they are first fetched from global memory to local shared memory, and then the pattern is calculated based on the values in shared memory.

Asynchronous execution is a famous way to improve the performance of CUDA programs. The pipeline of CUDA is usually divided into three steps: 1) memory copy from host to device; 2) kernel execution; and 3) memory copy from device to host. In synchronous execution mode, if the step 1) or 3) is running, the kernel is idle. In contrast, when the kernel is running, the memory bus is idle. To parallelize the memory copy and kernel execution, double buffer and two CUDA streams are used one for memory copy and the other for kernel execution. When the kernel is processing the image data in the first buffer, the copy stream is used to transfer new image data into the second buffer. When the kernel is finished, the pointers of buffer are swapped and the kernel is restarted.

TABLE II
SPEED COMPARISON AMONG CPU-SILTP, STGC, MTGC [17], AND GPU-SILTP-BASED OBJECT SEGMENTATION METHODS

Sequence	Resolution	CPU-SILTP (fps)	STGC (fps)	MTGC (fps)	GPU-SILTP (fps)
Outdoor [17]	320×240	73.9	29.9	147.6	1036.2
Park1 [17]	352×288	53.6	25.2	106.8	833.6
Street	704×576	13.7	5.1	21.2	292.2

We compared the speeds of the CPU-SILTP-based, GC-based [17] and GPU-SILTP-based object segmentation methods at an eight-cores 2.66-GHz computer with Nvidia GeForce GTX 285 (the same device used in other experiments of this paper). The results are shown in Table II. The CPU-SILTP method is implemented in single-thread mode. Both the single-thread (STGC) and multithread GC (MTGC)-based methods are evaluated, and the number of threads used in MTGC is set to be 8, as in [17]. From Table II, we can see that the speed of CPU-SILTP is ∼1 time faster than STGC. Moreover, we can find that the speedup ratio between GPU-SILTP and CPU-SILTP consistently surpasses 10 and increases with pixel resolution. Finally, we can see that the speedup ratio between GPU-SILTP and MTGC consistently surpasses 7 and also increases with pixel resolution.

2) Multicore-Based Object Stitching: The modified Poisson editing method [11] is used to achieve the smooth stitching and can be seen as a problem of solving the linear equations [11]

$$\mathbf{A}\mathbf{x} = \mathbf{b} \tag{12}$$

where $\mathbf{A}$ is a large, sparse and known $p \times p$ matrix, and p denotes the processing pixel number; the column vector $\mathbf{x}$ denotes the p unknown pixel values, and $\mathbf{b}$ is a known column vector for the Poisson equation. Therefore, our goal is to find a fast solution for (12).

Konstantinidis and Cotronis [28] proposed a parallel red–black successive over-relaxation method to fast solve (12), based on GPU with CUDA. The key idea of this parallel method is to divide the unknown variables $\mathbf{x}$ into a red set and a black set according to their coordinates, then parallelly update the values of each set in turn at each iteration with GPU. However, the GPU resource has been assigned to accelerate the moving object segmentation as mentioned before, therefore, to avoid the competition for the GPU resource, the multicore parallel technique is used. Thus, the OpenMP [29] programming is used to parallelly update the values of each set in turn at each iteration. Table III shows the comparison of stitching time between solving (12) with and without OpenMP. It can be found that the speedup increases with the processing pixel number. This inspires us to combine object stitching jobs of several frames as a whole linear equation to be solved.

TABLE III
STITCHING TIME COMPARISON BETWEEN WITH AND WITHOUT OPENMP

Pixel Num.	Iter.	OMP. (ms)	No OMP. (ms)	Speed-Up
5994 × 3	5000	725.13	202.27	3.6
13229 × 3	5000	1608.44	350.57	4.6
56899 × 3	5000	6868.79	1319.49	5.2
82925 × 3	5000	22590.12	1808.46	12.5

D. Tube Reallocation

Rearranged tubes can be reallocated to further improve the solution for the optimization problem of (5). The idea is to reassign optimal start-time labels of the tube set $\boldsymbol{Q}' - \boldsymbol{Q}''$, where $\boldsymbol{Q}'$ is a set, including rearranged tubes in current stepwise and $\boldsymbol{Q}''$ is a set, including tube tails of the previous stepwise. A tube tail is often caused by the fact that the frame length of the tube is longer than the frame length of the $L1$ condensation space (Fig. 8). In this case, the start-time label of $\boldsymbol{Q}''$ must be set as 1 to keep chronological order of tubes. Therefore, tube reallocation only process tubes that from $\boldsymbol{Q}'$ to $\boldsymbol{Q}''$.

In practice, the system randomly selects a tube from $\boldsymbol{Q}'$ to $\boldsymbol{Q}''$ and treats it as an incoming tube, then recalculates it's optimal start-time label with (8). Because there does not exist tubes to be processed all the time, tube reallocation can be applied to the online video condensation at idle time. As a result, the proposed system can obtain a better solution without decelerating the processing speed. Fig. 10 shows a comparison of a typical process of the online video condensation with and without tube reallocation, where the same parameters are applied. We can find that before being full, the $L1$ condensation space accepts more tubes by the tube reallocation, which suggests that tube reallocation is helpful for improving condensation ratio.

IV. EXPERIMENTS AND ANALYSIS

The proposed system was evaluated with extensive experiments. Nine surveillance video sequences taken from indoor and outdoor scenes are used. The details of the running environment and the system setup are listed in Tables IV and V, respectively. During the whole evaluation process, the proposed system does not do any down sample operation for input videos. In the following, the performance of the proposed system is summarized in five aspects: 1) speed; 2) condensation ratio; 3) content-aware ability; 4) memory usage; and 5) visual quality. The results and condensed videos are reported on a project Web site: http://www.cbsr.ia.ac.cn/users/jqzhu/hpvcs.htm.

A. Speed

The results of speed are summarized in Table VI. The speed decreases with the increase of the pixel resolution. For the video sequence Overpass [10] with the smallest pixel resolution, the processing speed of the proposed system achieves 995.00 frames/s. For those video sequences with 320 × 240 resolution, the processing speed ranges from 531.99 to 662.57 frames/s. For those video sequences with 352 × 288 resolution, the processing speed is ∼390 frames/s.

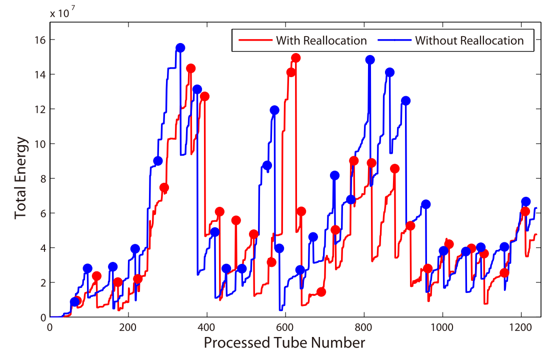

Fig. 10. Comparison between the online video condensation with and without tube reallocation for a typical tube filling process. The dots in the figure denote the moment when the $L1$ condensation space is full.

TABLE IV
DETAILS OF THE RUNNING ENVIRONMENT

Operating System	Window Server 2008 R2 Enterprise 64 bit
Hardware	CPU: 2.66 GHz 8 cores, GPU: Nvidia GeForce GTX 285
Compiler	Microsoft Visual Studio 2010

TABLE V
SYSTEM SETUP

Parameter	value
the frame length n of the $L1$ condensation space (Fig. 7)	500
the maximal tolerable threshold τ (Eq. (9))	1.0
the maximum temporary list size m (II-E3)	16
the length of tube buffer (Fig. 9)	200
the length of rearranged tube buffer (Fig. 9)	1

The processing speed of the proposed system is ∼5 times as faster as that reported in [17]. Even for those high-resolution (704 × 576) video sequences, the proposed system still has 100 frames/s that is three times faster than real-time (25 frames/s). Besides, as shown in Fig. 11, the time cost of the whole process is mostly determined by the tube generation thread. This result demonstrates that the time cost of the tube arrangement thread and the object stitching thread is well hidden, thus our multithread-based system is a very effective parallel system.

To show the speed advantage of online tube filling, the time cost of the online and offline tube filling algorithms was compared under the same hardware condition. Both of these two tube filling algorithms use greedy search (8) and the frame number of condensed video used in offline tube filling is equal to that in online tube filling. From Fig. 12, it can be found that the online tube filling is faster than offline tube filling. Especially, when the number of frames in an input video is huge (Outdoor, Street, and T-junction cases in Fig. 12), the running time of the online tube filling is only 6.53% to 20.10% of the offline tube filling. Because the longer the input video is, the larger the saturated count k of the $L1$ condensation space will be, resulting in the larger speedup ratio between the online and the offline tube filling according to (11).

B. Condensation Ratio

Condensation ratio (CR) is defined as the ratio between the number of frames in an input video and the number of

TABLE VI
RESULTS OF THE ONLINE CONTENT-AWARE VIDEO CONDENSATION SYSTEM ON NINE SURVEILLANCE VIDEO SEQUENCES

Video	Resolution	#Frame	Tube Num.	Speed (fps)	CR	AMU (MB)	PMU (MB)
Overpass [10]	320 × 120	23950	60	995.00	23.85	91.27	133.00
Exit [17]	320 × 240	81538	361	608.17	22.15	186.13	276.00
Garden [17]	320 × 240	33826	142	662.57	35.06	58.55	81.00
Outdoor [17]	320 × 240	138556	1181	531.99	8.20	475.47	733.00
Park1 [17]	352 × 288	10221	44	390.43	9.26	92.29	111.00
Passage	352 × 288	51040	20	390.36	34.96	134.75	316.00
Street	704 × 576	100113	521	100.39	15.83	777.30	1155.00
Staircase	704 × 576	46108	495	100.62	10.25	310.44	732.00
T-junction	704 × 576	600001	1418	106.71	36.76	513.67	1366.00

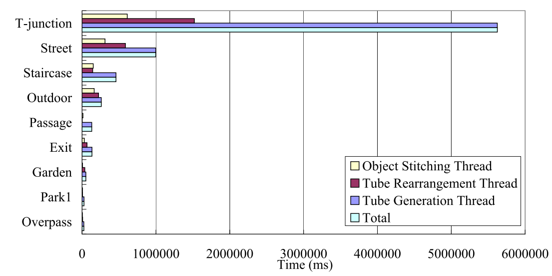

Fig. 11. Time cost of the three threads on nine video sequences.

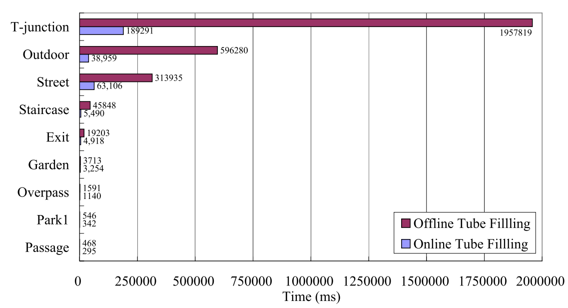

Fig. 12. Running time comparison between the online and the offline tube filling.

frames in the condensed video. The results of condensation ratio are summarized in Table VI. In Table VI, the lowest condensation ratio is 8.20, whereas the highest one is 36.76. Because the most existing methods have not reported condensation ratio results, we only compare our method with the ribbon carving-based method [10]. The proposed method has higher condensation ratio on the overpass sequence, ∼8 times (the condensation ratio reported in [10] is <3 for the overpass sequence). Moreover, the condensation ratio of the propose method can be easily adjusted by setting the maximum temporary list size m to different values. Comparing Fig. 13(b)–(d), we can find that our method can produce condensed videos with denser activities than the ribbon carving-based method [10].

C. Content-Aware Ability

The nine surveillance videos were processed automatically without any manual intervention. As shown in Table VI, the condensation ratio varies with different input video sequences, which demonstrates that our system has a content-aware ability

Fig. 13. Comparison of the proposed method versus the ribbon carving-based method [10]. (a) One frame from Overpass video. (b) Results by [10]. (c) and (d) Results by the proposed method with the maximum temporary list size $m = 8$ and $m = 16$, respectively.

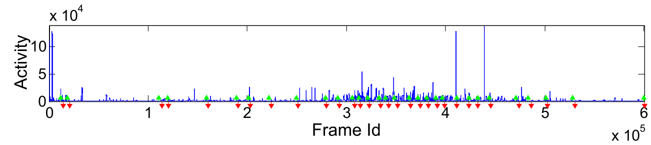

Fig. 14. Content-aware ability in the T-junction video sequence condensation process. The blue line represents the activity at each frame. Each red nabla in the figure denotes the moment that the $L1$ condensation space is full and green delta denotes the updating moment of the background image used for object stitching.

to adaptively control condensation ratio. Fig. 14 intuitively exhibits the content-aware ability of our system. As shown in Fig. 14, from 3×10^5 to 4×10^5th frame, there are more activities in this period and the $L1$ condensation space is saturated more frequently. Besides that, in this period, more background images are used for object stitching, which is the desiring property of the background image selection. The content-aware ability is more desirable and reasonable than setting a fixed condensation ratio as in video synopsis [11], because users usually do not know the activity density of an input video beforehand.

D. Memory Usage

The average memory usage (AMU) and peak memory usage (PMU) are summarized in Table VI. In Table VI, even for those high-resolution (704 × 576) input video sequences, the peak memory usage of our system is <1.5 GB. In addition, for the T-junction sequence with 600 001 frames, its memory usage status over time is plotted in Fig. 15. Combining Figs. 14 and 15, we can find two situations: 1) the memory usage is low and changes smoothly from 1×10^5 to 3×10^5th frame where the activity is sparse and 2) the memory usage firstly increases and then decreases from 3×10^5 to 4×10^5th frame, where the activity is dense. This is because the online processing mechanism makes the system use less memory in the activity sparse period and the two producer–consumer parallel models (Fig. 9) make our system is able to limit the memory usage when the consumption speed lower than the production speed in the activity dense period. Therefore, our system is suitable for endless input videos.

E. Visual Quality

For object-level recall rate, both the proposed system and our previous work [17] are able to condense all moving

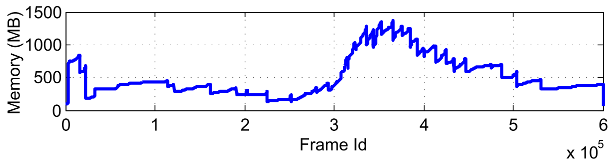

Fig. 15. Memory usage status in the condensation process of T-junction.

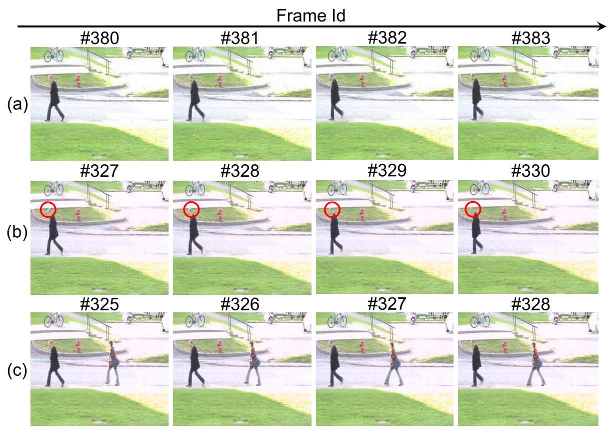

Fig. 16. Visual quality comparison on the pedestrians [22] sequence. (a) Input video. (b) Condensed video produced by [11] and red circles point out the missing parts. (c) Condensed video produced by the proposed method.

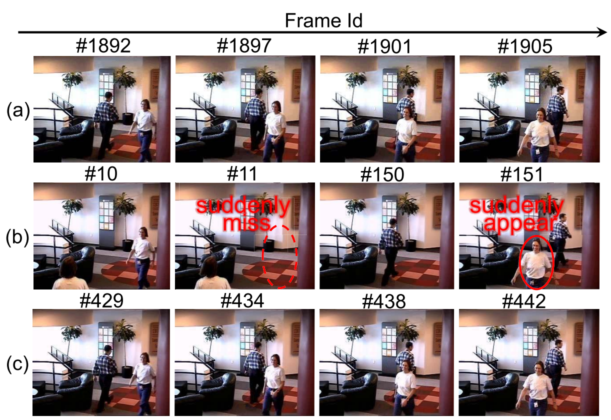

Fig. 17. Visual quality comparison on the IndoorGTTest1 [30] sequence. (a) Input video. (b) Condensed video produced by [11]. (c) Condensed video produced by the proposed method.

objects into the condensed video due to the online content-aware strategy. However, the method in [11] has a chance of discarding some moving objects in the synopsis video due to fixed synopsis video length and occlusion conflict. For pixel-level recall rate, as shown in Table I, the SILTP-based moving object segmentation method used in our system achieves higher recall rate than the GC-based object segmentation method used in [17], thus the recall rate of the proposed system is higher than that in [17]. Note that [11] used a similar GC-based object segmentation method as in [17].

We further made a visual quality comparison between the proposed method and the video synopsis method [11] on two public sequences, pedestrians [22], and IndoorGTTest1 [30], as shown in Figs. 16 and 17. The IndoorGTTest1 [30] sequence was captured in indoor scene, whereas the pedestrians [22] was captured in outdoor scene with a poorer imaging quality. The numbers of frames in the condensed videos produced by the two methods were set equal. Because the video synopsis method [11] uses a color and GC-based moving object segmentation method, it has a chance of over-segmentation when the color of a moving object is similar to background. From Fig. 16, we can see that the man (the color of the head region is similar to background) in the condensed video is more completely segmented by the texture feature (SILTP)-based method than that of [11]. Furthermore, from Fig. 17, we can find that the proposed system can correctly keep the chronological order of moving objects because of the sticky tracking strategy, whereas the method of [11] has a blinking effect [moving objects suddenly appear or miss in two consecutive frames, Fig. 17(b)] due to tracking failure. Therefore, the propose method achieves better visual effect than [11].

V. Conclusion

A high-performance video condensation system based on an online content-aware video condensation framework has been proposed in this paper. The online framework can process input videos and produce condensed videos simultaneously, with much less memory and higher speed than the offline framework. Besides that, the online framework can automatically determine the duration of a condensed video. The high-performance video condensation system is designed using the multithreading technique. The proposed system further applies GPU and multicore techniques to accelerate the processing speed. The extensive experiments have shown the superiorities of the proposed system.

References

[1] D. O'Callaghan and E. L. Lew, "Method and apparatus for video on demand with fast forward, reverse and channel pause," U.S. Patent 5 477 263, Dec. 19, 1995.

[2] M. A. Smith and T. Kanade, "Video skimming and characterization through the combination of image and language understanding techniques," in *Proc. IEEE CVPR*, Jun. 1997, pp. 775–781.

[3] N. Petrovic, N. Jojic, and T. S. Huang, "Adaptive video fast forward," *Multimedia Tools Appl.*, vol. 26, no. 3, pp. 327–344, 2005.

[4] B. Höferlin, M. Höferlin, D. Weiskopf, and G. Heidemann, "Information-based adaptive fast-forward for visual surveillance," *Multimedia Tools Appl.*, vol. 55, no. 1, pp. 127–150, 2011.

[5] M. M. Yeung and B.-L. Yeo, "Video visualization for compact presentation and fast browsing of pictorial content," *IEEE Trans. Circuits Syst. Video Technol.*, vol. 7, no. 5, pp. 771–785, Oct. 1997.

[6] X. Zhu, X. Wu, J. Fan, A. K. Elmagarmid, and W. G. Aref, "Exploring video content structure for hierarchical summarization," *Multimedia Syst.*, vol. 10, no. 2, pp. 98–115, 2004.

[7] C. Kim and J.-N. Hwang, "An integrated scheme for object-based video abstraction," in *Proc. 8th ACM Int. Conf. Multimedia*, 2000, pp. 303–311.

[8] Y. Li, T. Zhang, and D. Tretter, "An overview of video abstraction techniques," HP Lab., Palo Alto, CA, USA, Tech. Rep. HPL-2001-191, 2001.

[9] H.-W. Kang, X.-Q. Chen, Y. Matsushita, and X. Tang, "Space-time video montage," in *Proc. IEEE CVPR*, Jun. 2006, pp. 1331–1338.

[10] Z. Li, P. Ishwar, and J. Konrad, "Video condensation by ribbon carving," *IEEE Trans. Image Process.*, vol. 18, no. 11, pp. 2572–2583, Nov. 2009.

[11] Y. Pritch, A. Rav-Acha, and S. Peleg, "Nonchronological video synopsis and indexing," *IEEE Trans. Pattern Anal. Mach. Intell.*, vol. 30, no. 11, pp. 1971–1984, Nov. 2008.

[12] Y. Pritch, A. Rav-Acha, A. Gutman, and S. Peleg, "Webcam synopsis: Peeking around the world," in *Proc. IEEE 11th ICCV*, Oct. 2007, pp. 1–8.

[13] A. Rav-Acha, Y. Pritch, and S. Peleg, “Making a long video short: Dynamic video synopsis,” in *Proc. IEEE CVPR*, Jun. 2006, pp. 435–441.

[14] Y. Pritch, S. Ratovitch, A. Hendel, and S. Peleg, “Clustered synopsis of surveillance video,” in *Proc. IEEE Int. Conf. Adv. Video Signal Based Surveill.*, Sep. 2009, pp. 195–200.

[15] M. Xu, S. Z. Li, B. Li, X. Yuan, and S. Xiang, “A set theoretical method for video synopsis,” in *Proc. Multimedia Inf. Retr.*, 2008, pp. 366–370.

[16] S. Kasamwattanarote, N. Cooharojananone, S. Satoh, and R. Lipikorn, “Real time tunnel based video summarization using direct shift collision detection,” in *Advances in Multimedia Information Processing*. Berlin, Germany: Springer-Verlag, 2010, pp. 136–147.

[17] S. Feng, Z. Lei, D. Yi, and S. Z. Li, “Online content-aware video condensation,” in *Proc. IEEE CVPR*, Jun. 2012, pp. 2082–2087.

[18] S. Liao, G. Zhao, V. Kellokumpu, M. Pietikainen, and S. Z. Li, “Modeling pixel process with scale invariant local patterns for background subtraction in complex scenes,” in *Proc. IEEE CVPR*, Jun. 2010, pp. 1301–1306.

[19] S. Feng, S. Liao, Z. Yuan, and S. Z. Li, “Online principal background selection for video synopsis,” in *Proc. IEEE 20th Int. Conf. Pattern Recognit.*, Aug. 2010, pp. 17–20.

[20] J. Sun, W. Zhang, X. Tang, and H.-Y. Shum, “Background cut,” in *Proc. ECCV*, 2006, pp. 628–641.

[21] C. Stauffer and W. E. L. Grimson, “Adaptive background mixture models for real-time tracking,” in *Proc. IEEE CVPR*, Jun. 1999, pp. 246–252.

[22] (2014). *A Video Database for Testing Change Detection Algorithms*. [Online]. Available: http://www.changedetection.net

[23] A. Yilmaz, O. Javed, and M. Shah, “Object tracking: A survey,” *ACM Comput. Surv.*, vol. 38, no. 4, 2006, Art. ID 13.

[24] T. Yang, S. Z. Li, Q. Pan, and J. Li, “Real-time multiple objects tracking with occlusion handling in dynamic scenes,” in *Proc. IEEE CVPR*, Jun. 2005, pp. 970–975.

[25] G. Brostow and I. Essa, “Motion based decompositing of video,” in *Proc. ICCV*, 1999, p. 8.

[26] W. Stallings, *Operating Systems: Internals and Design Principles*, 7th ed. Englewood Cliffs, NJ, USA: Prentice-Hall, Mar. 2011.

[27] *CUDA C Best Practices Guide*, NVIDIA, Santa Clara, CA, USA, 2012.

[28] E. Konstantinidis and Y. Cotronis, “Accelerating the red/black SOR method using GPUs with CUDA,” in *Parallel Processing and Applied Mathematics*. Berlin, Germany: Springer-Verlag, 2012, pp. 589–598.

[29] B. Chapman, G. Jost, and R. Van Der Pas, *Using OpenMP: Portable Shared Memory Parallel Programming*, vol. 10. Cambridge, MA, USA: MIT Press, 2008.

[30] L. M. Brown *et al.*, “Performance evaluation of surveillance systems under varying conditions,” in *Proc. IEEE PETS Workshop*, Jan. 2005, pp. 1–8.

Jianqing Zhu received the B.S. degree in communication engineering and the M.S. degree in communication and information systems from the School of Information Science and Technology, Huaqiao University, Xiamen, China, in 2009 and 2012, respectively, and the Ph.D. degree from the Institute of Automation, Chinese Academy of Sciences, Beijing, China, in 2015.

He is currently a Lecturer with the Faculty of Software, Fujian Normal University, Fuzhou, China. His research interests include computer vision and pattern recognition, with a focus on video analysis and video surveillance.

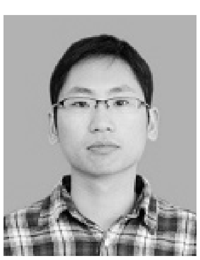

Shikun Feng received the B.S. degree in computer science and technology from the School of Computer, Wuhan University, Wuhan, China, in 2009 and the M.S. degree in pattern recognition and intelligent system from the Institute of Automation, Chinese Academy of Sciences, Beijing, China, in 2012.

His research interests include computer vision, pattern recognition, recommendation system, and user modeling.

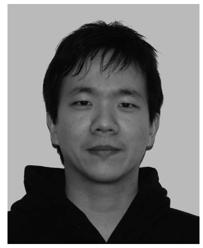

Dong Yi received the B.S. degree in electronic engineering and the M.S. degree in communication and information system from Wuhan University, Wuhan, China, in 2003 and 2006, respectively, and the Ph.D. degree in pattern recognition and intelligent systems from the Institute of Automation, Chinese Academy of Sciences, Beijing, China.

He developed the face biometric modules and systems for the immigration control projects and 2008 Beijing Olympic Games. His research interests include unconstrained face recognition, heterogeneous face recognition, and deep learning.

Shengcai Liao (M’13) received the B.S. degree in mathematics and applied mathematics from Sun Yat-sen University, Guangzhou, China, in 2005 and the Ph.D. degree from the Institute of Automation, Chinese Academy of Sciences (CASIA), Beijing, China, in 2010.

He was a Post-Doctoral Fellow with the Department of Computer Science and Engineering, Michigan State University, East Lansing, MI, USA, from 2010 to 2012. He is currently an Assistant Professor with CASIA. His research interests include face recognition and video analysis.

Zhen Lei (M’11) received the B.S. degree in automation from University of Science and Technology of China, Hefei, China, in 2005 and the Ph.D. degree from Institute of Automation, Chinese Academy of Sciences (CASIA), Beijing, China, in 2010.

He is an Associate Professor with CASIA. He has authored over 80 papers in international journals and conferences. His research interests include computer vision, pattern recognition, image processing, and face recognition.

Dr. Lei is the Area Chair of the 2014 International Joint Conference on Biometrics, the 2015 IAPR/IEEE International Conference on Biometrics, and the 2015 IEEE International Conference on Automatic Face and Gesture Recognition.

Stan Z. Li (F’09) received the B.Eng. degree from Hunan University, Changsha, China; the M.Eng. degree from National University of Defense Technology, Changsha; and the Ph.D. degree from Surrey University, Surrey, U.K.

He was an Associate Professor with Nanyang Technological University, Singapore. He was with Microsoft Research Asia, Beijing, as a Researcher from 2000 to 2004. He is currently a Professor and the Director of the Center for Biometrics and Security Research with the Institute of Automation, Chinese Academy of Sciences, Beijing, China. He has authored over 200 papers in international journals and conferences, and authored and edited eight books. His research interests include pattern recognition and machine learning, image and vision processing, face recognition, biometrics, and intelligent video surveillance.